Electroabsorption spectroscopy of effective-mass $Al_xGa_{1-x}As/GaAs$ Fibonacci superlattices

M. Dinu and D. D. Nolte
Department of Physics, Purdue University, West Lafayette, Indiana 47907-1396

M. R. Melloch
School of Electrical and Computer Engineering, Purdue University, West Lafayette, Indiana 47907-1285
(Received 3 March 1997)

Effective-mass Fibonacci superlattices are composed of quasiperiodic sequences of weakly coupled quantum wells in which the transfer-matrix element is significantly smaller than the confinement energy, which is significantly smaller than the confining potential. We identify several distinct classes of quasiperiodic superlattices that are distinguished by diagonal vs off-diagonal quasiperiodicity and by compositional vs structural quasiperiodicity. The spatial quasiperiodicity in Fibonacci superlattices leads to a fractal set of critical points in the one-electron spectra. In the hierarchy of quasiband critical points, the critical points associated with earlier generations are dominant and terminate the widest quasigaps. The interplay of the one-electron critical points with many-electron excitonic enhancements creates complex spectra. Excitonic interactions concentrate the oscillator strength to the lower-energy transitions, and exciton linewidths of late-generation critical points are broadened by Fano resonance with the continua of lower-energy critical points. Using electromodulation spectroscopy, we identify the first several generations of critical points in experimental absorption and electroabsorption spectra of several Fibonacci superlattices that differ in their structure and coupling strength. [S0163-1829(97)06327-3]

I. INTRODUCTION

Semiconductor multilayer structures are typically composed of two or more distinct semiconductor compounds that occur in periodic or aperiodic sequences. The possible combinations that can be made using modern growth techniques, such as molecular-beam epitaxy or related epitaxial growth techniques, are almost limitless. Therefore, this large design space has been broken into broad classes that encompass certain common properties. These classes include multiple-quantum-well (MQW) structures,[1,2] coupled quantum-well and resonant-tunneling structures,[3] and superlattices.[4,5] The key feature that distinguishes among these classes is the degree of quantum mechanical coupling from layer to layer. Quantum wells are isolated by wide barriers; coupled quantum wells consist of groups of wells that are coupled closely among themselves, but are otherwise isolated; superlattices consist of layers that are all coupled.

Within the class of superlattices, two limiting cases can be distinguished. Superlattices consisting of single monolayers or small numbers of monolayers are strongly coupled layer by layer. The electronic structure of these materials require first-principles calculations to accurately describe their electronic properties.[6–8] The other extreme case is the limit of weakly coupled quantum wells. Quantum wells consisting of many monolayers of low-gap material, and separated from other wells by many monolayers of higher-gap materials, can be weakly coupled by quantum-mechanical tunneling through the barriers. This class of superlattice can be viewed perturbatively as a tight-binding system within an effective-mass approximation. This considerably simplifies the theoretical understanding of the electronic structure of these superlattices, making heuristic models easily accessible to the experimentalist.

Also within the class of semiconductor superlattices are aperiodic structures that are composed of random or quasiperiodic sequences of layers. These structures have rich electronic spectra[9] that arise from wave-function localization. One well-known set of quasiperiodic superlattices are the Fibonacci superlattices.[10] These superlattices produce a fractal density of states, which has been studied in some detail in the case of strong-coupling superlattices.[11–13] Much less work has been performed on weak-coupling Fibonacci superlattices,[14] and little effort has been made to classify distinct forms of these weak-coupling superlattices. The weak-coupling Fibonacci superlattices possess a rich (but relatively unexplored) design space because of the flexibility in the use of variable widths and variable compositions in the well and barrier layers.

In this paper, we define and experimentally investigate two types of quasiperiodicity that are implemented with two types of disorder. The quasiperiodicity can be either diagonal or off-diagonal, and the quasiperiodicity can be implemented using either structural or compositional disorder. These different types of weak-coupling Fibonacci superlattices exhibit different spectra. In Sec. II we set the framework for the classification of various types of quasiperiodic and aperiodic heterostructures, describe the structures we have studied experimentally, and present a model for the calculation of the electroabsorption spectra. Section III presents the modulation spectroscopy experiments, and Sec. IV concludes with a discussion of the results.

II. FIBONACCI SUPERLATTICES

A. Fibonacci structure

A Fibonacci superlattice is a quasiperiodic heterostructure consisting of building blocks arranged in the Fibonacci sequence, which follows the rule that finite generations of the sequence are constructed by concatenating the two previous finite parent generations:

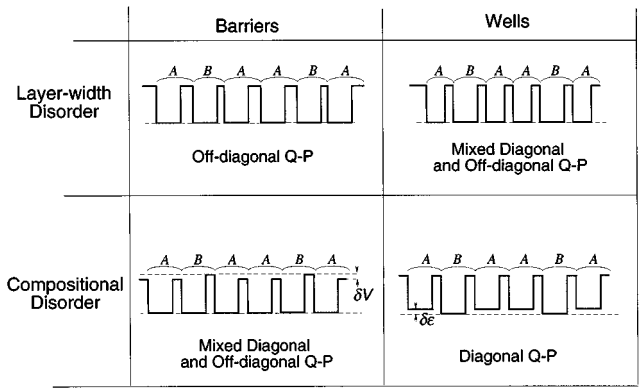

FIG. 1. Illustration of the classes of superlattice quasiperiodicity (Q-P) as a function of the type of disorder (diagonal or off-diagonal) when the quasiperiodicity is structural or compositional arising from perturbation of the wells or the barriers.

$$S_{N+1}=\{S_N S_{N-1}\}.$$

Each building block is made up of two types of terms or ''periods,'' which consists of a well and barrier of given thicknesses and Al fractions. In the case that the wells have a longer and shorter width, the Fibonacci superlattice would be represented as the sequence of well widths: *LSLLSLSLLSLLS*, etc.

To facilitate the description of various types of Fibonacci superlattices, one can make a distinction between diagonal and off-diagonal quasiperiodicity, based on the manner in which the quasiperiodicity affects the electronic spectrum of the Fibonacci superlattice. In diagonal quasiperiodic lattices, the on-site energies deviate from periodicity, while in off-diagonal quasiperiodic lattices the on-site energies are periodic but the site-to-site transfer or hopping energies are quasiperiodic. In semiconductor superlattices, spatial quasiperiodicity can be due to layer-width disorder or compositional disorder, which both lead to different types of quasiperiodicity depending on whether they affect the superlattice barriers or wells. In the approximation of first-order terms in the perturbation from periodicity, the influence of both types of disorder on the superlattice quasiperiodicity is schematically depicted in Fig. 1.

The distinction between diagonal and off-diagonal perturbations on a lattice is important in the case when the perturbation is random (pure disorder), where it leads to distinct mobility edge[15] behavior with increasing disorder.[16] It can also influence the emergence of van Hove-type critical points at the center of the energy band.[17] One-dimensional systems with either diagonal or off-diagonal disorder are always localized,[18] while the states in systems with diagonal or off-diagonal quasiperiodicity seem to be critical.[19] However, there may be special cases in off-diagonal quasiperiodic systems when at least one state is extended.

The Fibonacci superlattices (FSL's) we have studied (described below) fall approximately into the two categories of quasiperiodicities we have defined here. One of the structures (FSL No. 2) is an off-diagonal Fibonacci superlattice due to barrier-width quasiperiodicity. Two other structures were mainly diagonal Fibonacci superlattices: FSL No. 3, due to compositional quasiperiodicity in the wells and barrier-width quasiperiodicity; and FSL No. 4, due to well-width quasiperiodicity.

B. One-electron energy spectra of Fibonacci superlattices

We will illustrate the electronic properties of Fibonacci superlattices by considering a tight-binding (Kronig-Penney) approach,[20] which is a valid approximation for long-period superlattices because the coupling between wells is small enough to be considered a perturbation of the isolated well wave functions. The coupling between two wells in the superlattice sequence i and j is described by the transfer $t_{ij}=\langle i|V_i|j\rangle$ and shift $s_{ij}=\langle i|V_j|i\rangle$ integrals, where $|i\rangle$ is the isolated well wave function, and V_i is the superlattice potential corresponding to well i. Therefore, the one-carrier tight-binding Hamiltonian[20] can be written in the form

$$H=\sum_{i,j}(\varepsilon_i\delta_{ij}+s_{ij})|i\rangle\langle i|+\sum_{i,j}t_{ij}|j\rangle\langle i|, \tag{1}$$

where ε_i are the isolated well energy levels. This takes an average over the crystal potential of the superlattice in the form of a series of potential step functions, while the band-structure details are only taken into account through the carrier effective masses. The deviation from a periodic superlattice can be quantitatively characterized by the variations along the superlattice in the transfer and shift integrals δt_{ij} and δs_{ij}. The departure from a periodic superlattice treatment consists of solving the Hamiltonian for all N wells of the superlattice, with the isolated quantum-well wave functions as the basis, and considering only nearest-neighbor well-to-well interaction. Therefore such a model does not take into account band nonparabolicities, valence-band mixing, and electron correlation effects. A simple one-carrier approach to the calculation of the electron or hole minibands can extract the prominent energy distribution features of the experimentally observed transitions. However, many interesting characteristics such as oscillator strength can only be approached in the framework of a many-body treatment[21] of excitonic effects.

Any quasiperiodic spatial variation in the superlattice, such as quasiperiodic interwell coupling or confinement energy, will induce a fractal distribution of allowed energy states in the reciprocal space. If spatial quasiperiodicity is introduced starting from a periodic superlattice, then the superlattice minibands will acquire a fractal distribution of minigaps which define ''quasibands.'' The one-dimensional one-carrier density of states therefore resembles a ''devil's staircase,'' and quasiband edges are indicated by sharp slopes in the density of states.

Representative devil's staircases are shown in Fig. 2 for both diagonal and off-diagonal quasiperiodicity. The most important aspect of the devil's staircase density of states is the distribution of quasigaps of increasing number and decreasing size. The notable difference in the gap distribution between the case of diagonal and off-diagonal quasiperiodicity is the asymmetry with respect to the center of the band in the first case, and the symmetry in the later case. In off-diagonal quasiperiodicity, symmetry about the center of the band is a consequence of the diagonal degeneracy and the hermiticity of the tight-binding Hamiltonian; it can be de-

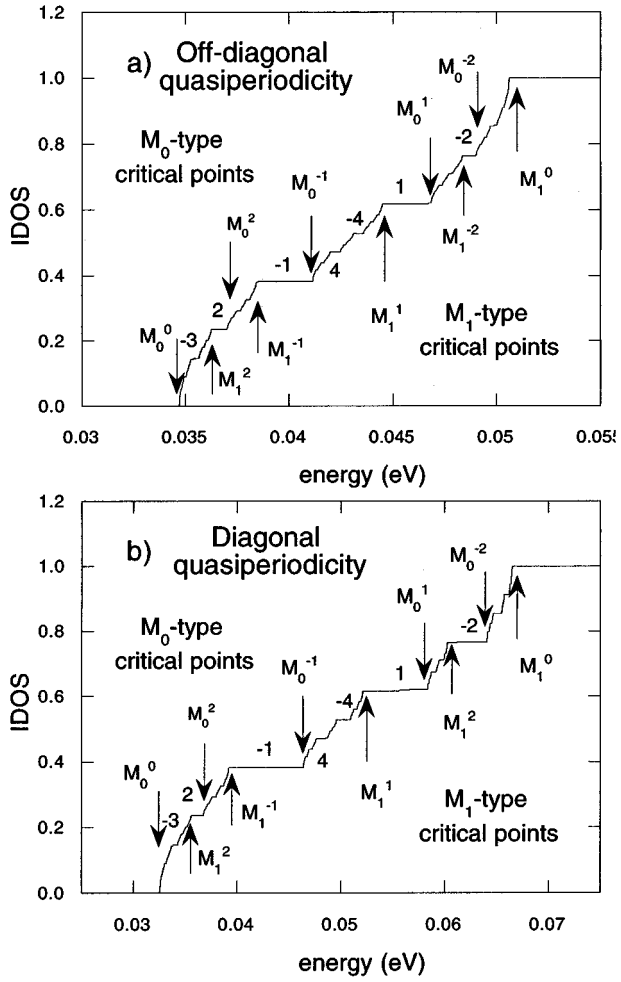

FIG. 2. Illustration of the hierarchy of critical points in quasibands for off-diagonal and diagonal superlattice quasiperiodicity. The curves are the calculated integrated one-electron density of states for (a) off-diagonal Fibonacci SL No. 2 and (b) diagonal Fibonacci SL No. 4. The subscripts designate the type of critical point (van Hove singularity), while the superscripts label the generation of the quasigap associated with the critical points, as discussed in the text.

scribed as perturbing a periodic lattice by introducing quasiperiodic coupling. The asymmetry in the case of diagonal quasiperiodicity, on the other hand, is not strictly a consequence of the coupling; it arises due to a perturbation on an initially quasiperiodic lattice. For decreasing coupling, the limiting situations in the two cases are quite different. In the limit of no coupling (very thick barriers), an off-diagonal superlattice is indistinguishable from that of the isolated quantum well. On the other hand, in the same limit a diagonal quasiperiodic superlattice exhibits a two-level spectrum that preserves the occupation ratio due to the quasiperiodic spatial arrangement of the now isolated wells.

C. Transition hierarchy and critical-point nomenclature

The greatest challenge for optical spectroscopy of Fibonacci superlattices is the correct identification of the many optical transitions that are observable in modulation spectroscopy. In general, N periods of the superlattice produce N distinct optical transitions. When N is large ($N=100$ in our case) this presents a formidable task. Fortunately for the spectroscopist, not all transitions have equal strength. In fact, there is a hierarchy of modulation signatures that make it sufficient to identify only a few of the critical point transitions in order to describe most of the modulation spectra. This hierarchy is based on the iterative generation of quasigaps by successive Fibonacci generations.

The magnitude of the quasigaps plays an important role in the modulation spectroscopy of the Fibonacci superlattices. Each gap terminates a quasiband at an M_1 saddle point, and begins a quasiband at an M_0 critical point.[22] Many-electron effects, such as excitonic enhancements in the absorption, are concentrated at M_0 critical points. There are several ways in which the quasigaps act to augment the electroabsorption, through modifications of the excitonic Rydberg, and through the broadening mechanism of Fano resonance.[23]

The largest quasigaps are associated with the largest Fourier components of the quasiperiodic potential, which also provides the largest effective mass to the associated M_0 critical point. The larger effective mass produces a larger exciton Rydberg and a larger oscillator strength, which gives a stronger modulation signal during modulation spectroscopy. Therefore the larger quasigaps will produce larger modulation signatures. The hierarchy of decreasing gap sizes is expected to produce a hierarchy of diminishing modulation signatures.

In addition to the effects on excitonic oscillator strength, each discrete M_0 excitonic transition is degenerate with the continuum of each lower-energy transition. This condition may produce Fano resonance, in which the transition probability of the continuum states interferes with the resonance, producing broadening of the transition linewidth. The M_0 critical points that terminate the larger quasigaps experience smaller broadening because of smaller interaction with the underlying continua. Smaller gaps, on the other hand, allow a greater interaction with the continua and therefore a larger broadening. Since broadening implies smaller modulation signals, the hierarchy of diminishing quasigap sizes will again produce a hierarchy of diminishing modulation signatures.

The hierarchy of diminishing modulation signatures considerably simplifies the task of identifying the many transitions observed experimentally in a Fibonacci superlattice, because the strongest modulation signatures will be associated with the M_0 transitions of the larger quasigaps. For a given experimental line-shape resolution, it may be necessary to identify only the first several M_0 critical points in order to describe the strongest modulation features of the Fibonacci spectrum.

This hierarchy also suggests an unambiguous nomenclature scheme for identifying the transitions based on the rank of the gap. The nomenclature scheme shown in Fig. 2 is based on the well-known trifurcation of the Cantor set spectrum of the one-dimensional Fibonacci chain.[19] Due to the scaling properties of the spectrum, each gap can be unambiguously labeled using an integer m, related to the quasiband occupation of the integrated density of states (IDOS) at the bottom of the gap,[24] which is $\{m\tau\}=m\tau-\mathrm{int}(m\tau)$, where the golden ratio $\tau=(\sqrt{5}-1)/2$. Generally, the gaps with lower index are larger and emerge in earlier Fibonacci

TABLE I. Structure of the three Fibonacci superlattices and of the periodic control superlattice.

	Layer *A*		Layer *B*	
Structure	well	barrier	well	barrier
Fibonacci SL No. 2	75-Å GaAs	25-Å $Al_{0.30}Ga_{0.70}As$	75-Å GaAs	18-Å $Al_{0.30}Ga_{0.70}As$
Fibonacci SL No. 3	75-Å $Al_{0.01}Ga_{0.99}As$	18-Å $Al_{0.30}Ga_{0.70}As$	75-Å GaAs	25-Å $Al_{0.30}Ga_{0.70}As$
Fibonacci SL No. 4	62-Å GaAs	16-Å $Al_{0.30}Ga_{0.70}As$	75-Å GaAs	16-Å $Al_{0.30}Ga_{0.70}As$
Periodic SL	62-Å GaAs	16-Å $Al_{0.30}Ga_{0.70}As$	62-Å GaAs	16-Å $Al_{0.30}Ga_{0.70}As$

generations. This nomenclature provides an unambiguous way of designating the multiple critical points in the superlattice. Each gap will be bracketed between an M_1-type critical point on the lower-energy side and an M_0-type critical point on the higher-energy side, both of which will be indexed by a superscript identifying the gap. This provides an exhaustive scheme for labeling the superlattice critical points. In the off-diagonal Fibonacci superlattice, the two largest gaps are degenerate in size. Each of these is identified as first generation gaps, followed by successive generation pairs of gaps. Although the density of states of the diagonal superlattice is asymmetric with respect to the center of the band, it follows the same scaling behavior, and its gaps can be designated by the same nomenclature scheme.

Using this nomenclature, it should possible to identify experimentally the first several generations of M_0-type critical points in a spectrum. The general trend is expected to be approximately valid, i.e., that the larger gaps will have associated with them the strongest modulation signatures. However, since this trend is based on a one-carrier treatment, it is expected to hold in general, but to fail in detail once electron-hole interaction effects are considered. In a periodic superlattice, the oscillator strength of the excitonic transitions in a miniband tends to concentrate strongly at the low-energy M_0 critical point.[21] We can expect many-body effects to produce the same tendency in a quasiperiodic superlattice. Therefore, the general aspect of the spectrum will be determined by the multifractal distribution of one-carrier critical points, but the strength of the transitions will be primarily influenced by many-electron effects, which will induce a bias in the spectrum, augmenting the low-energy transitions and broadening the higher-lying transitions in the quasiband. This preferential distribution of the oscillator strength at the low-energy critical points will determine the general appearance of the electrotransmission spectra.

III. MODULATION SPECTROSCOPY

We have experimentally investigated several different Fibonacci superlattices, together with a purely periodic superlattice as a control structure. In all structures the superlattice barriers are made of $Al_{0.3}Ga_{0.7}As$ and the superlattice consists of 100 periods. The off-diagonal superlattice FSL No. 2 has a quasiperiodic barrier-width sequence, of 25- and 18-Å barriers, the longer barriers being more numerous. In the mixed diagonal and off-diagonal structure FSL No. 3, in addition to a quasiperiodic barrier-width sequence (18- and 25-Å barriers, the shorter barriers being more numerous), compositional quasiperiodicity was incorporated into the wells by the introduction of 1% Al fraction in the more numerous wells. Growths FSL Nos. 2 and 3 both had 75-Å wells. In the diagonal structure FSL No. 4 the GaAs well widths are equal to either 62 or 75 Å (shorter wells are more numerous), with the barriers 16 Å wide. Finally, the periodic control superlattice (PSL No. 1) had 62-Å GaAs wells and 16-Å barriers. The building blocks for each of the superlattices are given in detail in Table I.

All structures were grown by molecular-beam epitaxy; an $Al_{0.5}Ga_{0.5}As$ layer was included to serve as a stop etch. The samples were epoxied onto glass slides and the substrates were removed using a wet chemical etch,[25] so that transmission measurements could be made. Gold contacts were evaporated onto each sample with a spacing of 1 mm to apply an electric field in the plane of the wells. The sample geometry is identical to the geometry of transverse-field photorefractive quantum wells.

Electroabsorption measurements at liquid helium temperatures were performed using a Janis Supervaritemp optical cryostat. An ac electric field was applied in the plane of the quantum wells up to fields as high as 4 kV/cm. The transmitted and electromodulated light were detected using a preamplified Si photodiode and lock-in detection, with the lock-in amplifier referenced either to a chopper or to the applied ac electric field.

An electric field applied parallel to the quantum wells (in the Franz-Keldysh geometry) induces a change in the transmission ΔT through exciton lifetime broadening or exciton ionization. The detected electromodulated signal is directly related to the change in absorption due to the applied electric field, and for small modulation the dependence is given by $\Delta T/T = L\Delta\alpha$, where L is the thickness of the semiconductor heterostructure and T is the zero-field transmission. Measuring the differential transmission $\Delta T/T$ therefore provides a way of determining the change in the absorption coefficient of the excitonic transition, which is directly correlated with the transition oscillator strength. The differential transmission is also the quantity of interest when using semiconductor heterostructures as photorefractive electrooptic modulators[14,26] for light diffraction and optical processing. For such applications, the diffraction efficiency is the most important parameter, and its magnitude and spectral dependence are determined by the magnitude and spectral dependence of the differential transmission.

Apart from the transition oscillator strength f, the change in absorption depends on the zero-field linewidth of the transition Γ_0, the variation of the linewidth $\Delta\Gamma(E)$ with the applied electric field E, and also on the saturation of the broadening with field. The electroabsorption depends on these factors as

$$\Delta\alpha(E) \propto f\Delta\Gamma(E)/\Gamma_0^2. \quad (2)$$

The excitonic oscillator strength f is a measure of the transition probability, and in the simplest model, in the approximation where carrier correlation effects are not taken into account, is quantified by the overlap of the conduction band and valence band carrier wave functions. The field-induced broadening describes the ionization enhancement of the exciton under an applied electric field. Qualitatively, the exciton ionization probability increases with increasing applied electric field, up to the point when $\Delta\Gamma(E)$ saturates. The zero-field linewidth of the transition Γ_0 depends on thermal broadening and on the interaction of the given transition with lower-lying continua (Fano resonance). In real systems, factors such as sample variations (well- or barrier-width fluctuations) or microscopic electric fields produced by material damage[27] can inhomogeneously increase the exciton linewidth.

Taking these factors into account, the general features of the electrotransmission spectrum can be described as follows. It has been shown that the excitonic oscillator strength tends to concentrate in the lower-energy part of the superlattice miniband.[28] Therefore, due to this preferential distribution of the oscillator strength, the strongest transition oscillator strengths will be associated with the lower-energy quasiband critical points. The increased interaction of the higher-energy critical points with lower continua will produce larger Fano broadening Γ_0 of these transitions. The field-induced broadening will also vary across the superlattice miniband; qualitatively, the excitons with lower binding energy will broaden and saturate faster than the higher-binding-energy excitons, associated with the critical points following the larger quasigaps. The combined effect of these factors will be that the sharpest and strongest transitions will occur at the lower energies in the miniband, and the higher-lying transitions will be weaker and broader.

A. Periodic superlattice

We examined a periodic superlattice structure, as a control for quantifying deviations from ideality due to growth effects such as interface roughness, and for the purpose of testing our numerical model on a relatively simple system. The absorbance and electroabsorption low-temperature spectra are shown in Fig. 3, with the predicted transition energies for the heavy- and light-hole excitons derived from the numerical model. The absorbance is defined as $\ln(1/T)/L$, where T is the transmission and L is the sample thickness, and is proportional to the absorption of the sample but does not take into account Fresnel reflections at interfaces. The calculations for all superlattices have been performed within a transfer-matrix approach,[13,29] using the nominal superlattice parameters, which have not been adjusted to provide a better fit. Table II shows the experimental transition energies, together with the calculated assignments. The transition energies have been given a rigid shift to align the fundamental transition energy with the lowest experimental transition. In calculating the transition energies, we have taken into account the strain introduced by the differential contraction of the glass substrate through a rigid shift of the gap, and an additional splitting of the light- and heavy-hole bands, estimated from known expansion coefficients and deformation potentials for GaAs and glass.[30,31] The heavy- and light-hole excitonic features dominate the sample. The saddle-type M_1 critical points for the light- and heavy-hole minibands appear as inflection points in the absorption spectrum, and there is good agreement with the predicted critical point energies. The spectra show that, within the resolution of our measurements (which ranges between 0.1 and 0.2 meV), there is no observable spectral structure due to layer fluctuations and interface roughness. Therefore we conclude that the longer periods of our Fibonacci superlattices render the spectral features relatively insensitive to small variations in layer widths. More sensitive techniques should be able to detect the spectral lines due to such factors.[32]

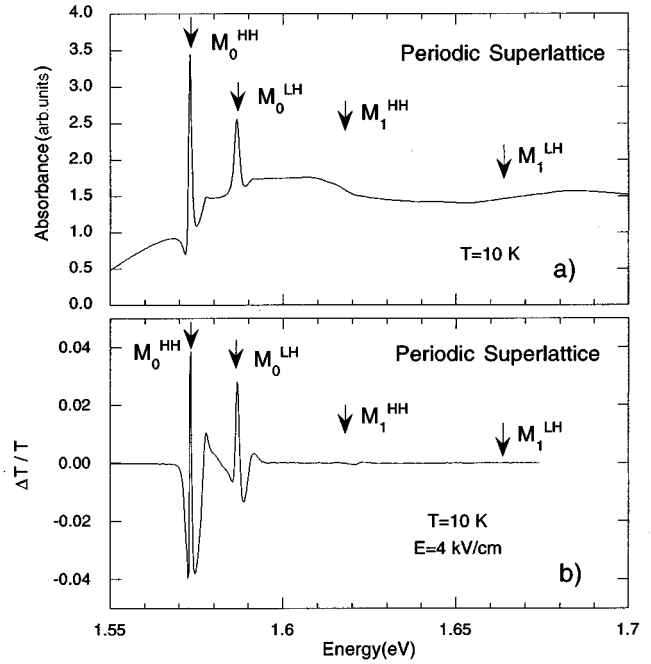

FIG. 3. Absorption (a) and differential transmission (b) spectra of the periodic control superlattice. The indicated critical points are calculated using the nominal parameters of the superlattice and no adjustable parameters, neglecting exciton effects.

The three Fibonacci superlattices we have studied go from off-diagonal to mainly diagonal quasiperiodicity, as can be seen from the quasiperiodic variation of the transfer and shift integrals among the superlattices (Table III). FSL No. 2 is

TABLE II. Critical points of the periodic superlattice heavy- and light-hole minibands. The calculations have used the nominal superlattice parameters, but the transition energies have been rigidly shifted to align the calculated and experimental fundamental transitions. The calculated energies have been corrected for the effects of strain but not for the exciton Rydberg.

Measured transition energy (eV)	Assignment label	Calculated transition energy (eV)
1.5733	$n=1$ HH M_0	1.5733
1.5867	$n=1$ LH M_0	1.5850
1.6219	$n=1$ HH M_1	1.6150
1.6558	$n=1$ LH M_1	1.6569
1.7340	$n=2$ HH M_1	1.7484

TABLE III. Characteristic energy variations in the four Fibonacci superlattices, with the notation from Eq. (1). The table shows the change in the respective energy between the two types of blocks in the superlattice. All energies are given in meV.

Structure	$\lvert\delta\varepsilon_i\rvert$	$\lvert\delta t_{ii}\rvert$	$\lvert\delta s_{ii}\rvert$
Fibonacci SL No. 2	0.0	2.21	0.33
Fibonacci SL No. 3	8.10	2.21	0.33
Fibonacci SL No. 4	11.74	5.73	0.38

almost purely off-diagonal, as characterized by the variation δt_{ij}, calculated to be ≈ 2.2 meV. The corresponding diagonal variation δs_{ij} is negligible, as in all the superlattices; however, in any real superlattice δs_{ij} can never be exactly zero, and therefore any real quasiperiodic superlattice has some degree of diagonal quasiperiodicity. For FSL No. 3 the diagonal term $\delta\varepsilon_i = 8.1$ meV is more significant than the transfer integrals; likewise, FSL No. 4 is strongly diagonal. This trend can also be perceived in the complexity of the measured spectra.

B. Off-diagonal quasiperiodicity

The absorption and electromodulation spectra for the off-diagonal Fibonacci superlattice FSL No. 2 are shown in Fig. 4. Also shown in the figure are the assigned transition labels, in accordance with the notation convention described in Sec. II C. The transition energies are calculated starting from the one-carrier quasibands in both the conduction and valence

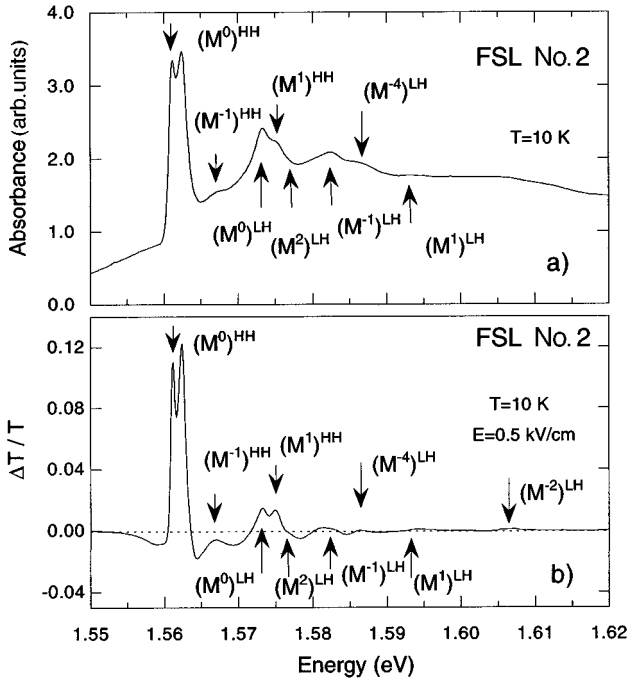

FIG. 4. The (a) absorption and (b) differential transmission spectra of the off-diagonally quasiperiodic Fibonacci superlattice FSL No. 2. The off-diagonal quasiperiodicity preserves the symmetry of the energy band, and leads to few prominent transitions. The transitions between major critical points in the quasiband are labeled following the convention introduced in Fig. 1(a).

TABLE IV. Critical points of the Fibonacci superlattice FSL No. 2. The calculated energies use the nominal superlattice parameters, but have been corrected through a rigid shift to account for deviations from the nominal thicknesses. The exciton binding energies have not been included in the calculated values.

Measured transition energy (eV)	Assignment label	Calculated transition energy (eV)
1.5612	HH M_0^0	1.5612
1.5624	HH M_0^{-3}, M_0^2	1.5621, 1.5633
1.5670	HH M_0^{-1}	1.5676
1.5732	LH M_0^0	1.5767
1.5749	HH M_0^1	1.5740
1.5767	LH M_0^2	1.5804
1.5826	LH M_0^{-1}	1.5877
1.5863	LH M_0^4	1.5902
1.5943	LH M_0^1	1.5992
1.6072	LH M_1^0	1.6094

bands. The correspondence between the measured and calculated transition energies is shown in Table IV. Transitions are assumed to take place between M_0 critical points in the conduction and valence bands. The transition energies do not include the exciton binding energies. Implicit in our assignments are ''selection rules'' that eliminate from consideration all but a few possible transitions. Even in a one-carrier approximation, the oscillator strength of a given transition can still be estimated from the overlap integrals of the corresponding electron and hole envelope functions.[33] Based on this analysis, we found that the strongest transitions occur mostly between equivalent (i.e., having the same rank in the gap hierarchy) M_0-type critical points in the energy quasibands. In this sense, the off-diagonal Fibonacci superlattice still approximately preserves the well-known $n = n'$ selection rule that is obeyed in the case of isolated quantum wells.

As can be seen from Fig. 4, the symmetry of the quasibands in the case of the off-diagonal superlattice leads to a relatively small number of transitions. This is a consequence of the simplicity of the symmetrical hierarchy.

C. Combined diagonal and off-diagonal quasiperiodicity

The electroabsorption and absorption spectra for the mixed diagonal and off-diagonal superlattice FSL No. 3 are shown in Fig. 5. The correspondences between the strongest transitions and the calculated transition energies are indicated, and the numerical values are shown in Table V. As in the case of FSL No. 2, the lowest-energy light-hole exciton transition is an adjustable parameter in the assignments. However, the lowest-energy light-hole transition can be unambiguously identified to occur at 1.578 eV by comparing the absorption spectra of a sample with biaxial strain with a strain-free (freestanding) sample. Unlike the case of the off-diagonal superlattice, the lack of inversion symmetry in the quasiband together with the increased superlattice coupling lead to the appearance of ''forbidden'' transitions, i.e., transitions between nonequivalent M_0-type critical points in the quasibands. For instance, the feature at 1.5713 eV is attributed to a transition between the M_0^0 critical point in the electron quasiband and the M_0^2 critical point in the heavy-hole

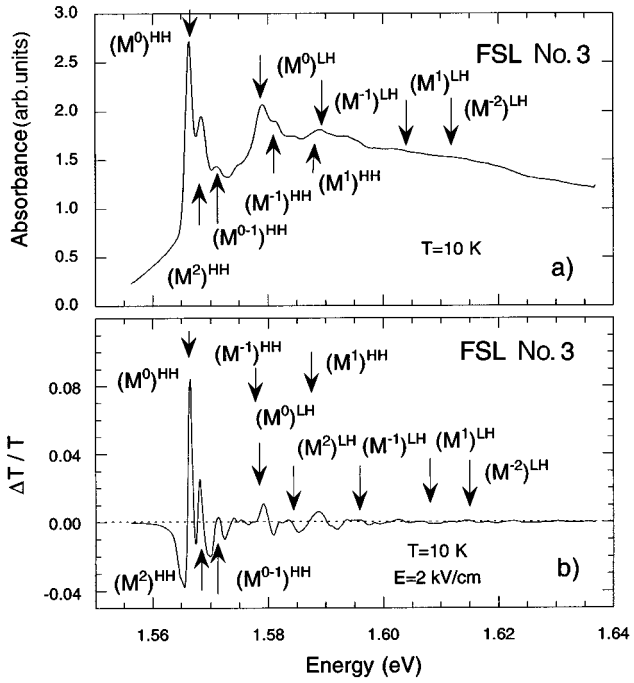

FIG. 5. The (a) absorption and (b) differential transmission spectra of the combined diagonal and off-diagonal quasiperiodic Fibonacci superlattice FSL No. 3. The important transitions are shown with their attributed critical points. The diagonal quasiperiodicity removes the symmetry of the quasiband density of states, and leads to a richer distribution of gaps evident in the spectra.

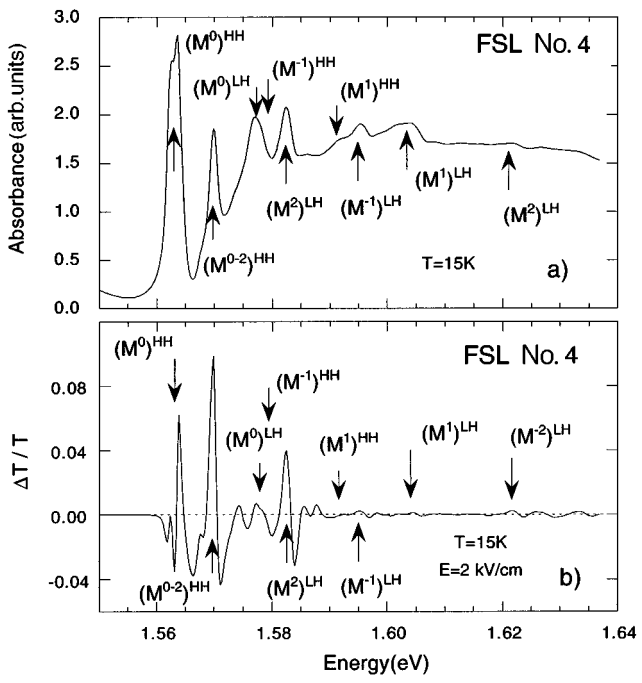

FIG. 6. The (a) absorption and (b) differential transmission spectra of the mainly diagonal quasiperiodic Fibonacci superlattice FSL No. 4. The large diagonal quasiperiodicity destroys the symmetry of the energy quasiband, and leads to a multitude of transitions of comparable intensity. The transitions between the main critical points in the quasiband are labeled following the designations of Fig. 2(c).

quasiband (labeled HH M^{0-2} in our notation). The agreement between the assignments and the observed transitions is good, also showing that in the case of this superlattice the one-carrier tight-binding treatment captures the distinctive features of the electromodulation spectra. The number of spectral features observed is larger due to a more complicated hierarchy in the density of states.

D. Strong diagonal quasiperiodicity

The strongly diagonal Fibonacci supperlattice FSL No. 4 is interesting because it exhibits both stronger interwell coupling and more pronounced quasiperiodicity compared with the other two Fibonacci superlattices. The absorption and electromodulation spectra for the FSL No. 4 superlattice are shown in Figs. 6(a) and 6(b). The spectra exhibit a large number of transitions, the most important of which are identified as described for the Fibonacci superlattice FSL No. 3. Table VI shows the transition assignments of the strongest experimental transitions. The hierarchy of critical points is similar in the two diagonal superlattices, and the identification of the salient transitions relies on the same oscillator strength arguments. A peculiarity of the Fibonacci superlat-

TABLE V. Critical points of the Fibonacci superlattice FSL No. 3. The calculated energies have used the nominal superlattice parameters but have been corrected through a rigid shift to account for deviations from the nominal thicknesses. The exciton binding energies have not been included in the calculated values.

Measured transition energy (eV)	Assignment label	Calculated transition energy (eV)
1.5665	HH M_0^0	1.5665
1.5675	HH M_0^2	1.5684
1.5713	HH M_0^{0-2}	1.5714
1.5772	HH M_0^{-1}	1.5788
1.5791	LH M_0^0	1.5824
1.5835	LH M_0^2	1.5860
1.5888	HH M_0^1	1.5868
1.5960	LH M_0^{-1}	1.5959
1.6067	LH M_0^1	1.6100
1.6145	LH M_0^{-2}	1.6174

TABLE VI. Critical points of the Fibonacci superlattice FSL No. 4. The calculated energies use the nominal superlattice parameters, but have been corrected through a rigid shift to account for deviations from the nominal thicknesses. The exciton binding energies have not been included in the calculated values.

Measured transition (eV)	Assignment label	Calculated transition energy (eV)
1.5639	HH M_0^0	1.5639
1.5698	HH M_0^{0-2}	1.5697
1.5773	LH M_0^0	1.5794
1.5825	LH M_0^2	1.5854
1.5919	HH M_0^1	1.5920
1.5954	LH M_0^{-1}	1.6002
1.6043	LH M_0^1	1.6219
1.6217	LH M_0^{-2}	1.6358

tice FSL No. 4 is the strong dependence of the spectral distribution of electromodulation intensity on applied field. The electroabsorption spectra corresponding to three different applied fields are shown in Fig. 7. The intensity of the electromodulation signal of the higher-energy transitions saturates for small applied electric fields. Also apparent in Fig. 6 is the sharpness of the lower-lying features, and especially that of the feature we attribute to the $(M^{0-2})^{HH}$ transition, occurring between the M_0^0 critical point in the electron quasiband and the M_0^{-2} critical point of the heavy hole quasiband; the sharpness is probably due to the absence of a continuum with which the transition energy can have a degeneracy. The interplay between the dependences of electric field sensitivity and linewidth on transition energy and the tendency of the oscillator strength to concentrate at the lower energies produces a complicated dependence of the modulated signal as a function of electric field across the energy quasibands.

IV. DISCUSSION

The guiding principle we have used in assigning transition labels to observed features in the electromodulation spectra is that complexity in a spectrum is inversely correlated with feature importance, i.e., the most prominent features are due to early generations of the Fibonacci superlattice, and features that appear in later generations have lower prominence in the spectrum. This principle follows naturally from the fractal nature of the energy spectrum, correlated with the previously discussed excitonic effects, broadening mechanisms, and electric-field sensitivity dependence, which all tend to relatively augment the low-energy critical points following larger quasigaps to the disadvantage of the higher-lying transitions or those following smaller quasigaps. The superlattices we have studied span different degrees of conformance to these principles. For the weaker coupling Fibonacci superlattices FSL No. 3 and especially FSL No. 2, these arguments seem to be valid because the lower-energy excitonic transitions, either light hole or heavy hole, always show higher electroabsorption. Also, as the field is increased, the relative intensities of the transitions do not change, indicating a slowly varying sensitivity to field across the quasibands. The heuristic arguments we have proposed begin to break down in the case of the stronger coupling diagonal Fibonacci superlattice FSL No. 4; the transitions in this superlattice show different field dependence and saturation across the quasibands.

To summarize, the fractal nature of the one-carrier energy quasibands gives rise to multiple critical points in the absorption and electroabsorption spectra. The dominant features are due to critical points in the one-carrier quasibands that emerge in low-order generations of the Fibonacci sequence, and their hierarchy can therefore be understood within a simple one-carrier model. The details of the electroabsorption spectrum are due to many-electron interactions, which determine the distribution of oscillator strength in the quasiband and augment the low-energy transitions. A helpful distinction can be made between diagonal and off-diagonal quasiperiodicity: the asymmetry of the diagonally disordered quasiband induces a more complicated distribution of gaps and critical points and leads to the relaxation of the selection rules obeyed in periodic and off-diagonal superlattices.

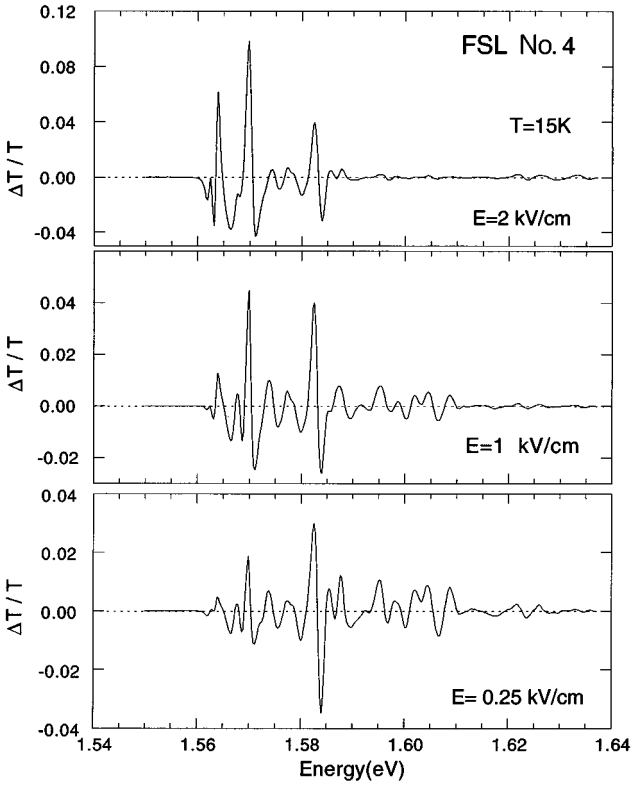

FIG. 7. The electroabsorption spectra at three different applied electric fields for the mainly diagonal quasiperiodic superlattice FSL No. 4. The interplay between sensitivity to field and oscillator strength produces a complicated field dependence of transition strengths across the quasiband.

[1] F. L. Lederman and J. D. Dow, Phys. Rev. B **13**, 1633 (1976).
[2] D. S. Chemla, Helv. Phys. Acta **56**, 607 (1983).
[3] V. I. Belyavsky, Y. V. Kopaev, and S. V. Shestov, Solid State Commun. **94**, 715 (1995).
[4] L. Esaki and R. Tsu, IBM J. Res. Dev. **14**, 61 (1970).
[5] A. Chomette, B. Deveaud, and F. Clerot *et al.*, J. Lumin. **44**, 265 (1989).
[6] G. Bastard, Phys. Rev. B **24**, 5693 (1981).
[7] G. Bastard and J. A. Brum, IEEE J. Quantum Electron. **QE-22**, 1625 (1986).
[8] G. A. Sai-Halasz, L. Esaki, and W. A. Harrison, Phys. Rev. B **18**, 2812 (1978).
[9] K. Hirose, D. Y. K. Ko, and H. Kamimura, J. Phys., Condens. Matter. **4**, 5947 (1992).
[10] R. Merlin, K. Bajema, and R. Clarke *et al.*, Phys. Rev. Lett. **55**, 1768 (1985).
[11] R. Merlin, IEEE J. Quantum Electron. **24**, 1791 (1988).
[12] F. Laruelle and B. Etienne, Phys. Rev. B **37**, 4816 (1988).
[13] D. Munzar, L. Bocaek, and J. Humlicek *et al.*, J. Phys., Condens. Matter. **6**, 4107 (1994).

[14] M. Dinu, D. D. Nolte, and M. R. Melloch, J. Appl. Phys. **79**, 3787 (1996).
[15] P. W. Anderson, Phys. Rev. **109**, 1492 (1958).
[16] P. D. Antoniou and E. N. Economou, Phys. Rev. B **16**, 3768 (1977).
[17] A. Brezini, Phys. Lett. A **147**, 179 (1990).
[18] C. M. Soukoulis and E. N. Economou, Phys. Rev. B **24**, 5698 (1981).
[19] M. Kohmoto, B. Sutherland, and C. Tang, Phys. Rev. B **35**, 1020 (1986).
[20] G. Bastard, *Wave Mechanics Applied to Semiconductor Heterostructures* (Halsted, New York, 1988).
[21] H. Chu and Y.-C. Chang, Phys. Rev. B **39**, 10 861 (1989).
[22] M. Okuyama, T. Nishino, and Y. Hamakawa, J. Phys. Soc. Jpn. **35**, 134 (1973).
[23] U. Fano, Phys. Rev. **124**, 1866 (1961).
[24] Y. Liu, X. Fu, and X. Deng *et al.*, Phys. Rev. B **46**, 9216 (1992).
[25] R. Williams, *Modern GaAs Processing Methods* (Artech, Boston, 1990).
[26] Q. Wang, R. M. Brubaker, and D. D. Nolte *et al.*, J. Opt. Soc. Am. B **9**, 1626 (1992).
[27] D. D'Avanzo, IEEE Trans. Electron Devices **ED-29**, 1051 (1982).
[28] H. Chu and Y.-C. Chang, Phys. Rev. B **36**, 2946 (1987).
[29] S.-H. Pan and S.-M. Feng, Phys. Rev. B **44**, 5668 (1991).
[30] F. H. Pollak, in *Strained-Layer Superlattices: Physics*, edited by T. P. Pearsall (Academic, New York, 1990), Vol. 32, pp. 17–53.
[31] P. Voisin, Surf. Sci. **168**, 546 (1986).
[32] C. Parks, A. K. Ramdas, and M. R. Melloch *et al.*, Phys. Rev. B **48**, 5413 (1993).
[33] B. Zhu, Phys. Rev. B **37**, 4689 (1988).